25th ABCM International Congress of Mechanical Engineering
October 20-25, 2019, Uberlândia, MG, Brazil

COB-2019-0672
OPTIMISATION OF A BETA-TYPE STIRLING ENGINE DISPLACER PISTON USING HYBRID ALGORITHM

Bryan Castro Caetano
Jose Arthur Gonçalves da Silva Teixeira
Matheus Ungaretti Borges
Oscar Ricardo Sandoval Rodrigues
Rudolf Huebner
Ricardo Poley Martins Ferreira
Programa de Pós Graduação em Engenharia Mecânica - Universidade Federal de Minas Gerais UFMG, Av. Pres. Antônio Carlos, 6627 - Pampulha, Belo Horizonte - MG, 31270-901
bcastrocaetano@gmail.com
jose.arthur.gst@gmail.com
matheusungaretti@gmail.com
osc.sandoval@hotmail.com
rudolf@demec.ufmg.br
poley@demec.ufmg.br,

Abstract. *This work aims to optimise the dimensions involving the displacer piston of a Beta-type Stirling engine using optimisation algorithms. A hybrid algorithm associated with the first-order Schmidt model was used to verify the influence of geometric parameters on the engine power. Because it is a first-order model, the Schmidt model makes some simplifications that make it difficult to study parameters such as the gap between the displacer piston and the cylinder. In this way, some considerations are made in such a way that it is possible to calculate the boundary conditions in a more precise way, as for example considering the choke effect when submitted to supersonic flows. The Schmidt model is implanted in a hybrid algorithm that combines genetic algorithm theory and sequential quadratic programming. It was possible to find the best values for the diameter, stroke and length of the displacer piston. Finally, a validation was performed with experimental values measured in a dynamometric bench, allowing to evaluate the results obtained by the optimisation.*

Keywords: *Stirling engine; Beta type; Algorithm optimisation; Hybrid algorithm; Schmidt model*

1. INTRODUCTION

The search for clean energy sources is one of the greatest challenges nowadays. Stirling engines have become topic of interest due to their ability to accept different kinds of heat source, achieving high efficiencies (Karabulut *et al.*, 2009). This ability comes from the operation principle of Stirling engines: the use of heat exchange with an external source through wall conduction in order to expand and compress a working gas, transforming the energy into mechanical work (Walker, 1973). This allows the use of various heat sources of energy from solids (biomass or coal), liquids (mineral oils or biofuels) and gaseous (biogas or hydrogen) to solar radiation and fuel cells (Kongtragool and Wongwises, 2003; Nishiyama *et al.*, 2007; Farra *et al.*, 2012; Rokni, 2013; Colmenar-Santos *et al.*, 2016). Furthermore, minimal levels of pollutant emissions can be achieved if a better control of the heat source in which these engines operate is granted (Darlington and Strong, 2005).

There are several applications of Stirling engines, being the most common in solar energy technologies. Stirling engines with solar concentrators (CSP-Stirling) are considered one of the most promising energy conversion systems in recent years (Cheng and Yu, 2011). Scientific literature shows that Stirling engines using solar concentrators can reach an efficiency of 30% in the conversion of solar energy in electric energy (Mancini *et al.*, 2003). Solar energy comes as one of the viable solutions to reduce global dependence on fossil fuels. It is estimated that 80% of world energy demand is dependent on hydrocarbons (Abbas *et al.*, 2011).

This work aims to optimise parameters of interest of a Beta-type Stirling engine. Mathematical models were combined with optimisation techniques to calculate the optimum dimensions to obtain maximum engine power and thermal efficiency. To validate the numerical method, experimental tests were carried out on a dynamometer bench where geometric parameters such as the displacer piston diameter were varied. In this way, the use of the Schmidt model associated with the hybrid optimisation algorithm can be evaluated.

2. Literature review

In Stirling engines, the heat is added and removed by conduction through the walls of the expansion and compression chamber respectively due to a differential temperature, generating work from the expansion and the compression of the working fluid (Kong *et al.*, 2004). Currently, Stirling engines have characteristics that distinguish them from other thermal machines. The most important difference is the Stirling theoretical thermodynamic cycle.

The theoretical Stirling cycle is based on the addition of isothermal heat by a hot source and isothermal heat rejection by a cold source. It consists of a series of four reversible processes: isothermal expansion, isovolumetric cooling, isothermal compression and isovolumetric heating. The regenerator is a component added to the engine which has the function of collecting part of the rejected heat by the previous cycle for the working fluid in the hot source (Çengel *et al.*, 2006).

Its main advantages are: thermal efficiency with ideal regeneration close to the Carnot cycle (Walker, 1980); power gain without the need to use high pressures and large volumes displaced by the power piston as in the Carnot cycle (Walker, 1980); higher mechanical efficiency when compared to other kind of engines under the same conditions of temperature, compression ratio, working fluid and external pressure (Senft, 1993). Figure 1 shows the steps and positioning of the pistons during the process.

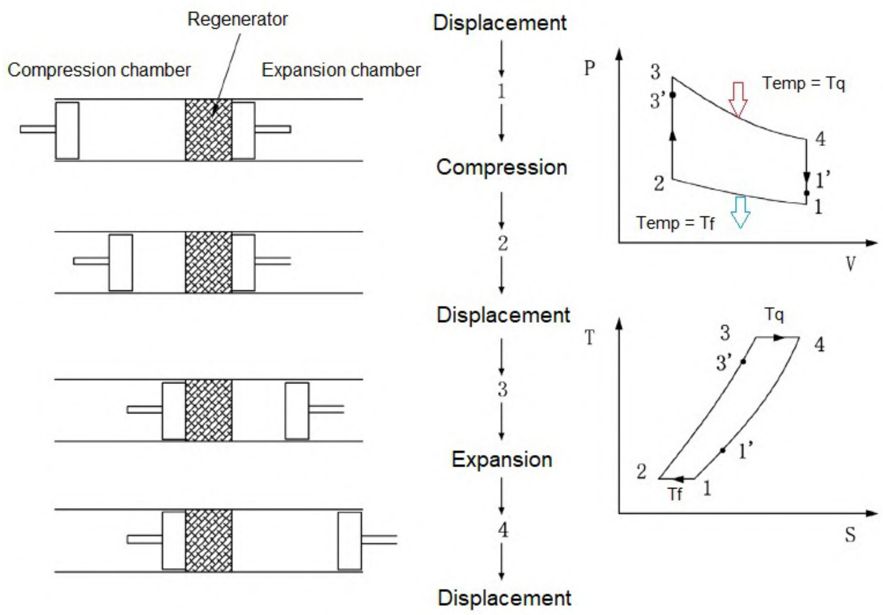

Figure 1: Stirling cycle illustration (Duan *et al.*, 2014).

The performance of a Stirling engine is susceptible to changes in geometric parameters such as piston stroke, displacer size and connecting rod lengths, and operating conditions as differential temperature between the expansion and the compression chambers, the type of fluid and the working pressure (Ahmadi *et al.*, 2017). The development of computational techniques and mathematical models is indispensable for the design and optimisation of the engine with a low computational cost and with a good precision (Hachem *et al.*, 2018). In the scientific literature, such models are defined according to their complexity as first-, second-, and third-order. The higher the order of the model, the higher is the computational cost for the solution (Paul and Engeda, 2015; Martini, 1978). Figure 2 shows an schematic drawing of a Beta-type Stirling engine.

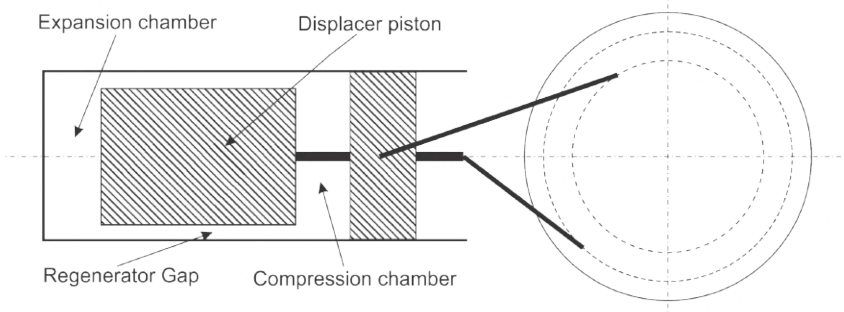

Figure 2: Schematic drawing of a Beta-type Stirling engine (Cheng and Yu, 2011).

2.1 Stirling Engine Modelling - Schmidt Analysis

The model proposed by Schmidt is the simplest isothermal calculation method for Stirling engines and it is useful for a first approximation. This model is based on isothermal expansion and isothermal compression of an ideal gas. From this model, Hirata (1997) presented some considerations for the calculation of pressure, shaft power and efficiency.

2.1.1 Pressure inside the Cylinder

The model proposed by Schmidt is the simplest isothermal calculation method for Stirling engines and it shows great utility for a first approximation. This model is based on isothermal expansion and compression of an ideal gas. For this, some considerations are made for the calculation of pressure, shaft power and efficiency (Hirata, 1997).

- The pressure drop in the heat exchangers and the internal pressure differences are neglected.
- The expansion and the compression processes are isothermal.
- The working fluid is considered an ideal gas.
- The regeneration is perfect.
- The dead space of expansion and compression maintains its temperatures during the cycle.
- The regenerator gas temperature is a mean of the hot and cold chamber gas temperature.
- The compression and expansion volumes vary sinusoidally.

The equations to calculate the instantaneous pressure inside the cylinder of a Beta-type Stirling motor used in this work are presented in Hirata (1997).

The ideal gas equation is shown in Eq. (1) .

$$pV = mRT \tag{1}$$

Using the ideal gas equation, the mass in a Stirling engine is shown in Eq. (2).

$$m = \frac{V_{se}p}{2RT_c} C - B\cos(x - A) \tag{2}$$

Being the values of A, B and C are given by Eqs. (3), (4) and (5), respectively.

$$A = \arctan\frac{v\sin(dx)}{t + \cos(dx) + 1} \tag{3}$$

$$B = \sqrt{T^2 + 2v(T-1)\cos(dx) + v^2 - 2T + 1} \tag{4}$$

$$C = t + 2tX_{de} + \frac{4tX_r}{1+t} + v + 2X_{dc} + 1 - 2X_b \tag{5}$$

in which, dx is the phase angle between the power piston and the displacer, t_d is the ratio between compression and expansion temperatures ($t_d = T_c/T_e$), v is the ratio between compression and expansion swept volumes ($v = V_{sc}/V_{se}$), X_{de} is the ratio between dead volume and expansion swept volume ($X_{de} = V_{de}/V_{se}$), X_{dc} is the ratio between compression dead volume and expansion swept volume ($X_{dc} = V_{dc}/V_{se}$), X_r is the ratio between regenerator volume and expansion swept volume ($X_r = V_r/V_{se}$) and X_b is the ratio between relative volume and expansion swept volume ($X_b = V_b/V_{se}$), in which, V_b is characterised by Eq. (8).

The volume of the expansion chamber V_e varies according to the rotation of the engine axis, its instantaneous value is given by Eq. (6).

$$V_e = \frac{V_{se}}{2}(1 - \cos(x)) + V_{de} \tag{6}$$

Like the expansion chamber, the compression chamber also varies in time. Equation (7) shows the value of the compression volume.

$$V_c = \frac{V_{se}}{2}(1 + c\cos(x)) + \frac{V_{sc}}{2}(1 - (\cos(x - dx))) + V_{de} \tag{7}$$

In a Stirling engine, both pistons are housed in the same cylinder. Therefore, when the pistons move, a relative volume of work is created. Equation (8) shows the value of the relative volume.

$$V_b = \frac{V_{se} + V_{sc}}{2} - \sqrt{\frac{V_{se}^2 + V_{sc}^2}{4} - \frac{V_{se} + V_{sc}}{2}\cos(dx)} \tag{8}$$

The instant total volume V is presented in Eq. (9).

$$V = V_e + V_r + V_c \tag{9}$$

The working pressure p_m is shown in Eq. (10).

$$p_m = \frac{2mRT_c}{V_{se}(C - B\cos(\theta - A))} \tag{10}$$

The pressure p inside the cylinder is given by Eq. (11)

$$p = \frac{p_m\sqrt{1 - \left(\frac{B}{C}\right)^2}}{1 - \cos(x - a)\left(\frac{B}{C}\right)} \tag{11}$$

2.1.2 Power and efficiency

In order to calculate the engine power, the estimation of the cycle work is necessary. Hence, it is necessary to discover the work received in the expansion of the working fluid and the work spent in the compression (Hirata, 1997). The engine power W_{net} can be calculated by the Eq.(12) as a function of the cycle net work and the engine speed n.

$$W_{net} = n(\tau_e - \tau_c) \tag{12}$$

in which, n is the engine speed, τ_e is the expansion work, τ_c is the compression work.
The engine efficiency (η_t) can be calculated by the Eq. (13)

$$\eta_t = 1 - \frac{T_c}{T_e} \tag{13}$$

in which, T_c is the compression chamber temperature and T_t is the expansion chamber temperature.
Equation (14) shows the work done by the gas during the expansion process.

$$\tau_e = \oint p dV_e = \frac{\pi p_m V_{se}\left(\frac{B}{C}\right)\sin(A)}{1 + \sqrt{1 - \left(\frac{B}{C}\right)^2}} \tag{14}$$

Equation (15) shows the work done by the gas during the expansion process.

$$\tau_c = \oint p dV_c = \frac{\pi p_m V_{sc}\left(\frac{B}{C}\right)\sin(A)}{1 + \sqrt{1 - \left(\frac{B}{C}\right)^2}} \tag{15}$$

2.1.3 Mach number

The Mach number M indicates whether the flow in a channel is subsonic, sonic or supersonic. Equation (16) shows how it is calculated.

$$M = \frac{V_f}{\sqrt{\gamma RT}} \tag{16}$$

in which, V_f is the fluid velocity, γ is the ratio of the heat capacity to the pressure constant and the heat capacity at constant volume, R is the gas constant and T is the fluid temperature.
in which, c is given by Eq. (17).

$$c = \sqrt{\gamma RT} \tag{17}$$

2.2 Optimisation Algorithm

Genetic algorithm (GA) is used to find the circa optimal solution of the problem. Once this region is found, then, a Sequential Quadratic Programming (SQP) is initiated for faster convergence to the local global optimum.

GA imitates nature's evolution model: subgroups of individuals are crossed and new offspring are created by genetic operators within a subpopulation. The selection of the best individuals is made every k generations and the best individual of a subpopulation is sent to its neighbours (Mühlenbein *et al.*, 1991).

There is no need to have a starting point provided by the user since the algorithm begins its search from a randomly generated population that evolves over successive generations. Three operators are used to propagate their population from one generation to another (Hassan *et al.*, 2005).

Working with a set (population) of vectors (individuals), the genetic algorithm is defined by three operators: "Selection", "Crossing" and "Mutation". The first operator imitates the principle of survival, whose objective is to select as severely as possible without destroying the diversity of the population. The second operator attempts to reproduce mating in biological populations. Thus, features of the best individuals of the current population are propagated to the next generation, improving the populational fitness value on average. The third operator promotes diversity in the characteristics of the population. The mutation operator allows global searching and prevents the algorithm from getting stuck in the ideal location (Hassan *et al.*, 2005). The mutation scheme works by sampling the neighbourhood exponentially more often than distant regions. When chosen, a bit of the selected individual is randomly chosen and inverted (Mühlenbein *et al.*, 1991).

SQP is a popular general purpose optimisation algorithm that creates an approximate quadratic programming subproblem that is used to find a search direction. However, the SQP algorithm may not converge to an optimal global if started away from a solution (Venter and Vanderplaats, 2009). This method replaces the original problem with a sequence of quadratic programming problems that are exactly solvable, approaching to the original. This is done by approaching the Lagrangian function by the second-order Taylor expansion at an initial point. For the formulation of the optimality conditions, the constraint functions are approximated by the first-order Taylor expansion. With the so-called active set strategy, it is possible to determine which constraints are to be included in the formulation in each quadratic problem of the Abdo and Rackwitz (1991) sequence.

The exact calculation of the second-order derivatives for the Hessian matrix is usually very expensive and cannot be efficiently implemented for a general case. In the first iteration, a unitary matrix is used instead of the true Hessian to solve the system of equations, and the solution of this quadratic problem with linear constraints defines a direction in which a line search is performed. This one-dimensional research is performed to obtain an ideal decrease of objective and constraint functions in that direction. The process for when the optimality conditions of the original problem are satisfied (Abdo and Rackwitz, 1991).

3. Methodology

The engine selected to be optimised was developed by Caetano (2018) and three different displacer piston diameters were tested. The obtained data will be used to observe how the engine performance varies with the displacer piston dimensions modification.

Three engine dimensions are optimised and they are connected directly with the displacer piston. Namely, the first is the displacer diameter, the second is the length and the third is the stroke.

The objective of the optimisation problem was to maximise the engine power, W_{net}, adjusting the dimensions of three parameters which are the displacer diameter D_d, the displacer stroke r_d and the displacer lenght H_d. For this, the objective function presented in Eq. (12) is used replacing the therms presented in Eqs. (14) and (15). Finally, the displacer geometry is limited by functional constraints, described by the Eq. (18).

$$\begin{cases} 0\,mm \leq D_d \leq 22.8\,mm \\ 20\,mm \leq r_2 \leq 40\,mm; \\ 10\,mm \leq H_d \leq 80\,mm \end{cases} \tag{18}$$

in which, D_d is the displacer diameter, r_2 is the displacer crank radius, H_d is the displacer length.

The Schmidt model does not limit the influence of the gap between the displacer piston and the cylinder wall. That is, with no gap, the highest power is obtained. However, this is not practicable since with no gap there is no exchange of mass between the chambers. Figure 3 shows the predicted power by varying the displacer diameter between 0 mm and 22.8 mm.

In order to analyse the influence of the displacer diameter, the choking condition of the flow through the gap between the displacer piston and the cylinder was added to the model. Therefore, the Mach number $M < 1$ was used as a boundary condition for the displacer diameter. The global optimisation algorithm was used to find the best value for each considered variable.

The engine selected to be optimised was the engine developed by Caetano (2018). The data obtained for three different

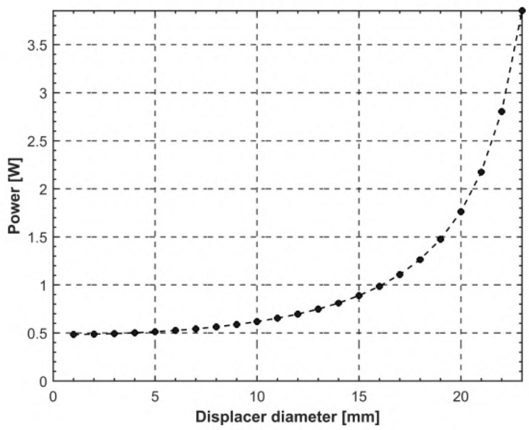

Figure 3: Displacer diameter influence on the shaft power by the Schmidt model.

displacer piston diameters will be used to observe and how the power of the engine varies with the variation of the dimensions of the displacer piston. Table 1 shows the engine main parameters: D_{dis} is the displacer diameter, V_{sc} is the swept volume of the power piston, V_{se} is the swept volume of the displacer piston, h_d is the displacer length, l_3 is the displacer connection rod length, r_1 is the power crank radius, r_2 is the displacer crank radius, l_1 is the length of the power piston linkage bar, l_2 length of the displacer piston linkage bar and the gap G between the displacer piston and the cylinder.

Table 1: Stirling engine characteristics.

Proprieties	Values
Engine Type	Beta
Bore	23 mm
r_1	12 mm
V_{sc}	9.79 cm^3
r_2	20 mm
V_{se}	13.59 cm^3
D_{dis} 1 - G	19.8 mm - 1.5 mm
D_{dis} 2 - G	20.8 mm - 1.0 mm
D_{dis} 3 - G	21.8 mm - 0.5 mm
h_d	116 mm
l_1	92.5 mm
l_2	54.7 mm
l_3	76.5 mm
Phase angle	90°
Working fluid	Air
Heating temperature	876 K and 676 K
Working pressure	93.2 kPa

A Beta-type Stirling engine prototype is developed for the experimental data collection, which are a basis for the Schmidt optimisation validation. The engine has a lubrication system to reduce friction, water cooling system to keep the temperature in the compression chamber constant (306 K) and uses it as heat source a natural gas combustion system for the expansion chamber. Figure 4 shows the geometric characteristics of the Stirling engine, with the instrumentation points (Caetano *et al.*, 2019).

4. Results

The results are divided in two parts. The first one is an analysis of the behaviour of each dimension individually. The second is an analysis of the behaviour of all the parameters together and the power and efficiency calculation.

Figure 5 shows the influence of the correction made on the length of the displacer piston relative to the output power of the engine for a piston of 21 mm in diameter and 41 mm stroke, original engine values. The correction added to the displacer length when evaluated in isolation showed that the smaller the displacement piston, the higher the power obtained. As the Schmidt model does not consider the influence of the regeneration made by the volume between the

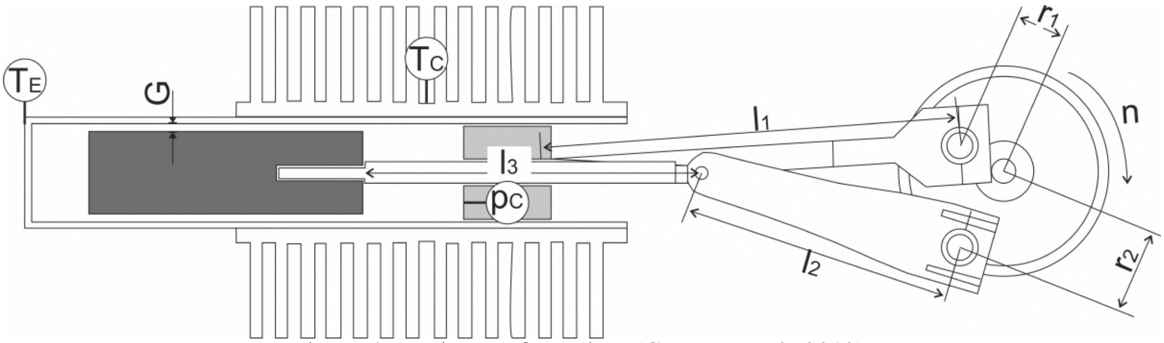

Figure 4: Engine configuration, (Caetano *et al.*, 2019).

displacer piston and the cylinder, decreasing the maximum length of the shifter is impractical.

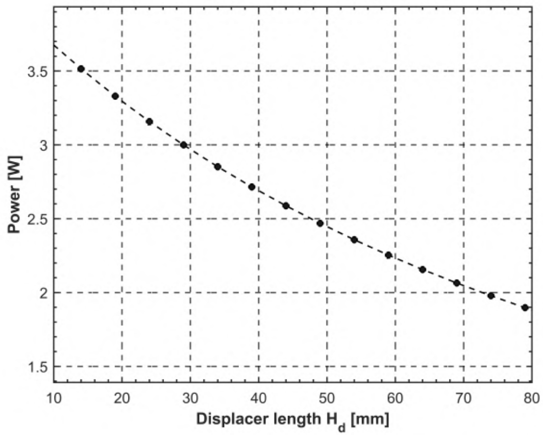

Figure 5: Power in function of displacer length correction.

The correction of the displacer course when analysed in isolation is shown in Fig. 6. It was observed a behaviour in the form of a parabola where the highest power is in corrections close to 30 mm. Figure 5 shows the influence of the correction made on the length of the displacer piston relative to the output power of the engine for a 21 mm diameter piston and 61 mm displacement length, original engine values.

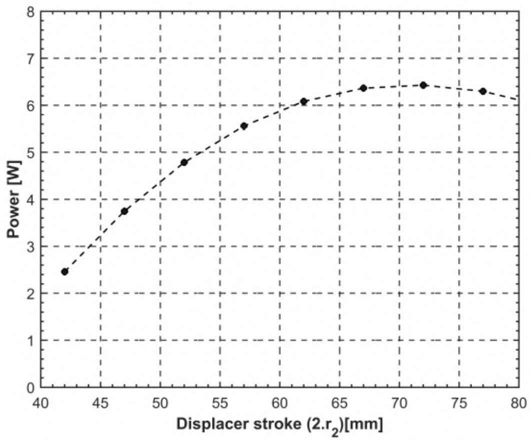

Figure 6: Power in function of displacement stroke correction.

The resultant surface on the influence of the displacer diameter and engine stroke on engine power is shown in Fig. 7. It is worth mentioning that the correction made in the course of the shifter is also made in the length of the shifter so that the dead volumes are kept the same.

Using as objective function the Eq. (12), together with the boundary conditions presented in the methodology section, an optimisation algorithm was implemented. As a result, the values for D_d, r_2 and h_d were obtained and presented in Tab. 2.

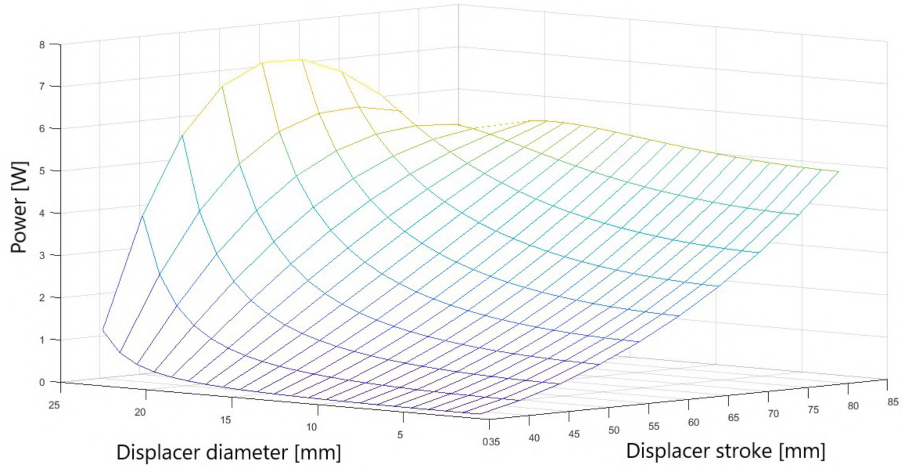

Figure 7: Influence of the displacer diameter in the power obtained by the Schmidt model.

In the Tab. 5 is possible to observe that the displacer length tends to be zero when analysed separately. However, as other parameters were evaluated together, it is possible to state that the displacer stroke value influences directly in the calculation of the optimal length and its value is not zero as shown in Tab. 2.

From Tab. 2 it is possible to observe that the optimisation algorithm used has zeroed the displacement length correction. This behaviour was expected, since as it was evaluated individually, the smaller the length of the displacer, the greater the power. In order to maintain the engine regeneration volume, only positive displacer correction values were considered in this study.

Table 2: Optimised values

Parameter	Dimension [mm]
D_d	21.34
r_2	31.80
h_d	35.40

It is worth mention that the theoretical power obtained by Schmidt model had higher error when compared with other theoretical models. This is due to the fact that Schmidt's model does not consider some existing processes in the engine, such as losses due to heat exchange between cylinder walls and fluid, friction losses and other inefficiencies. It is possible to observe that when the variables are optimised together different results are achievable when compared to the optimisation of the isolated variables.

It is noticeable that the optimisation algorithm calculates a small value for the displacer piston length. According to Schmidt's model, the thermal regeneration effects made by the displacer walls are not considered. Thus, with the smaller length is obtained the maximum power. It was decided not to work with values lower than 35 mm by a constructive limit.

Figure 8 shows the power for three different conditions: experimental power outputs, theoretical powers using the Schmidt model and the theoretical power for the optimised point using the methodology proposed in this work. The theoretical power was shown with a high error when compared with other theoretical models. This can be attributed to the fact that Schmidt's model does not consider some existing processes in the engine, such as losses due to heat exchange between cylinder walls and fluid and friction losses. Also, it is noticeable that when the variables are optimised together it is possible to achieve better results when compared to the optimisation of the isolated variables.

Finally, Fig. 9 presents and comparison with the Caetano (2018) engine in $A)$ and the engine with the optimised dimensions in $B)$. In the figure is possible to observe a great reduction in the displacer length. It is possible to affirm that the regeneration area was drastically reduted as well. It can be explained because the Schmidt model does not consider the influence of the gap between the displacer piston and the cylinder in the regeneration of the cycle.

5. Conclusions

Even with the Schmidt model limitations , which implies in a greater error margin, the corrections and boundary conditions added to the methodology presented in this work proved to be quite effective in optimising the three proposed variables. The chosen genetic algorithm was able to estimate realistic values and perfectly feasible in an engine design.

The diameter of the optimised displacer piston was close to the values tested. With this, it is possible to affirm that with the engine operating with the 22 mm piston, the flow between the displacer and the cylinder walls was chocked. This

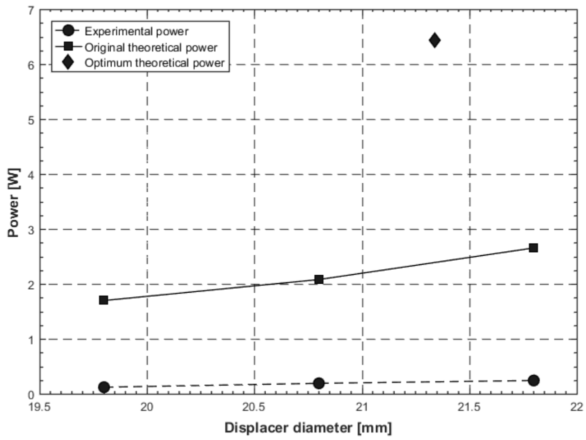

Figure 8: Shaft power for different geometric conditions.

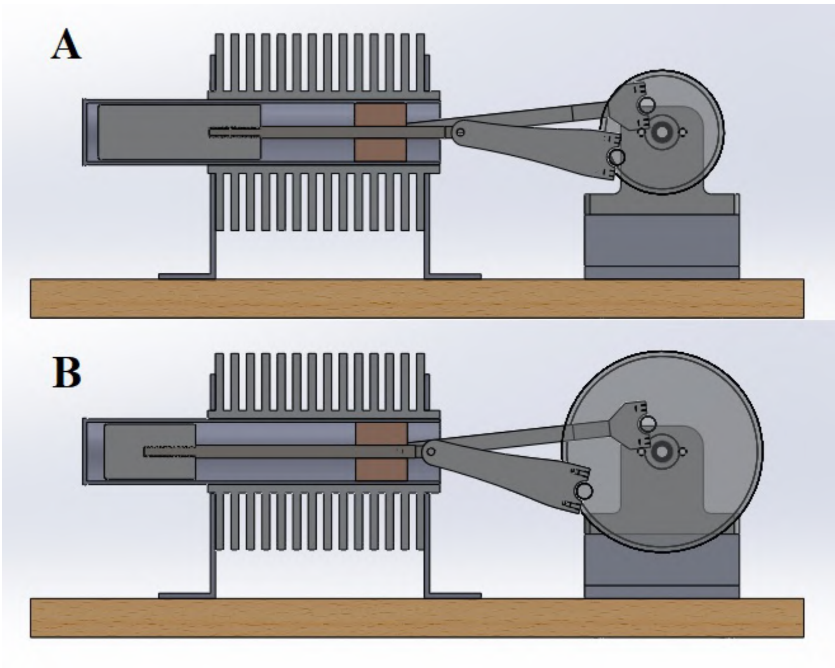

Figure 9: A) Original engine B) Optimised engine.

may have offered pumping losses and a decrease in engine performance.

The piston stroke correction proved to be the most influential variable in the output power of the engine. The correction found in the stroke of the displacer piston results in an optimum value of 67,6 mm travel of the displacer piston and a length of 35,4 mm. In this way, the dead volumes of expansion in compression were maintained, as well as the original compression ratio.

The methodology presented in this paper has proved possible for other variables to be studied in the future. As well, the genetic algorithm chosen can be used in other models that can offer results closer to the experimental values.

6. ACKNOWLEDGEMENTS

The authors acknowledge the Centro de Tecnologia da Mobilidade - CTM UFMG for providing the laboratory structure for this research, CNPq (142080/2019-5) for the financial support. This study was financed in part by the Coordenação de Aperfeiçoamento de Pessoal de Nível Superior - Brasil (CAPES) - Finance Code 001.

7. REFERENCES

Abbas, M., Boumeddane, B., Said, N. and Chikouche, A., 2011. "Dish stirling technology: A 100 mw solar power plant using hydrogen for algeria". *International journal of hydrogen energy*, Vol. 36, No. 7, pp. 4305–4314.

Abdo, T. and Rackwitz, R., 1991. "A new beta-point algorithm for large time-invariant and time-variant reliability problems". In *Reliability and Optimization of Structural Systems' 90*, Springer, pp. 1–12.

Ahmadi, M.H., Ahmadi, M.A. and Pourfayaz, F., 2017. "Thermal models for analysis of performance of stirling engine: A review". *Renewable and Sustainable Energy Reviews*, Vol. 68, pp. 168–184.

Caetano, B.C., 2018. "Estudo da influência das dimensões do pistão deslocador nos parâmetros de desempenho de um motor stirling do tipo beta". *Acta Mechanìca et Mobilitatem*, Vol. 2, No. 4, pp. 20–26.

Caetano, B.C., Lara, I.F., Borges, M.U., Sandoval, O.R. and Valle, R.M., 2019. "A novel methodology on beta-type stirling engine simulation using cfd". *Energy conversion and management*, Vol. 184, pp. 510–520.

Çengel, Y.A., Cimbala, J.M. and Sknarina, S.F., 2006. *Mecánica de fluidos: fundamentos y aplicaciones*, Vol. 1. McGraw-Hill.

Cheng, C.H. and Yu, Y.J., 2011. "Dynamic simulation of a beta-type stirling engine with cam-drive mechanism via the combination of the thermodynamic and dynamic models". *Renewable Energy*, Vol. 36, No. 2, pp. 714–725.

Colmenar-Santos, A., Zarzuelo-Puch, G., Borge-Diez, D. and García-Diéguez, C., 2016. "Thermodynamic and exergoeconomic analysis of energy recovery system of biogas from a wastewater treatment plant and use in a stirling engine". *Renewable Energy*, Vol. 88, pp. 171–184.

Darlington, R. and Strong, K., 2005. *Stirling and Hot Air Engines: Designing and Building Experimental Model Stirling Engines*. Crowood.

Duan, C., Wang, X., Shu, S., Jing, C. and Chang, H., 2014. "Thermodynamic design of stirling engine using multi-objective particle swarm optimization algorithm". *Energy Conversion and Management*, Vol. 84, pp. 88–96.

Farra, N., Tzanetakis, T. and Thomson, M.J., 2012. "Experimental determination of the efficiency and emissions of a residential microcogeneration system based on a stirling engine and fueled by diesel and ethanol". *Energy & Fuels*, Vol. 26, No. 2, pp. 889–900.

Hachem, H., Gheith, R., Aloui, F. and Nasrallah, S.B., 2018. "Technological challenges and optimization efforts of the stirling machine: A review". *Energy Conversion and Management*, Vol. 171, pp. 1365–1387.

Hassan, R., Cohanim, B., De Weck, O. and Venter, G., 2005. "A comparison of particle swarm optimization and the genetic algorithm". In *46th AIAA/ASME/ASCE/AHS/ASC structures, structural dynamics and materials conference*. p. 1897.

Hirata, K., 1997. "Schmidt theory for stirling engines". *Stirling Engine home page. Disponível em*.

Karabulut, H., Yücesu, H.S., Çınar, C. and Aksoy, F., 2009. "An experimental study on the development of a β-type stirling engine for low and moderate temperature heat sources". *Applied Energy*, Vol. 86, No. 1, pp. 68–73.

Kong, X., Wang, R. and Huang, X., 2004. "Energy efficiency and economic feasibility of cchp driven by stirling engine". *Energy Conversion and Management*, Vol. 45, No. 9-10, pp. 1433–1442.

Kongtragool, B. and Wongwises, S., 2003. "A review of solar-powered stirling engines and low temperature differential stirling engines". *Renewable and Sustainable energy reviews*, Vol. 7, No. 2, pp. 131–154.

Mancini, T., Heller, P., Butler, B., Osborn, B., Schiel, W., Goldberg, V., Buck, R., Diver, R., Andraka, C. and Moreno, J., 2003. "Dish-stirling systems: An overview of development and status". *Journal of Solar Energy Engineering*, Vol. 125, No. 2, pp. 135–151.

Martini, W.R., 1978. *Stirling engine design manual*. US Department of Energy, Office of Conservation and Solar Applications, Division of Transportation Energy Conservation.

Mühlenbein, H., Schomisch, M. and Born, J., 1991. "The parallel genetic algorithm as function optimizer". *Parallel computing*, Vol. 17, No. 6-7, pp. 619–632.

Nishiyama, A., Shimojima, H., Ishikawa, A., Itaya, Y., Kambara, S., Moritomi, H. and Mori, S., 2007. "Fuel and emissions properties of stirling engine operated with wood powder". *Fuel*, Vol. 86, No. 15, pp. 2333–2342.

Paul, C.J. and Engeda, A., 2015. "Modeling a complete Stirling engine". *Energy*. ISSN 03605442. doi:10.1016/j.energy.2014.11.045.

Rokni, M., 2013. "Thermodynamic analysis of sofc (solid oxide fuel cell)–stirling hybrid plants using alternative fuels". *Energy*, Vol. 61, pp. 87–97.

Senft, J.R., 1993. *Ringbom stirling engines*. Oxford University Press, USA.

Venter, G. and Vanderplaats, G., 2009. "Using a filter-based sqp algorithm in a parallel environment". In *50th AIAA/ASME/ASCE/AHS/ASC Structures, Structural Dynamics, and Materials Conference 17th AIAA/ASME/AHS Adaptive Structures Conference 11th AIAA No*. p. 2235.

Walker, G., 1973. *Stirling-cycle machines*. Clarendon Press.

Walker, G., 1980. *Stirling engines*. Oxford University Press, New York, NY.

8. RESPONSIBILITY NOTICE

The authors are the only responsible for the printed material included in this paper.